DOI: 10.1002/chem.200902259

Symmetrization of Cationic Hydrogen Bridges of Protonated Sponges Induced by Solvent and Counteranion Interactions as Revealed by NMR Spectroscopy

Mariusz Pietrzak,[a, e] Jens P. Wehling,[a] Shushu Kong,[a] Peter M. Tolstoy,[a, d] Ilya G. Shenderovich,[a, d] Concepción López,[b] Rosa María Claramunt,[b] José Elguero,[c] Gleb S. Denisov,[d] and Hans-Heinrich Limbach*[a]

Abstract: The properties of the intramolecular hydrogen bonds of doubly ^{15}N-labeled protonated sponges of the 1,8-bis(dimethylamino)naphthalene ($DMANH^+$) type have been studied as a function of the solvent, counteranion, and temperature using low-temperature NMR spectroscopy. Information about the hydrogen-bond symmetries was obtained by the analysis of the chemical shifts δ_H and δ_N and the scalar coupling constants J(N,N), J(N,H), J(H,N) of the $^{15}NH^{15}N$ hydrogen bonds. Whereas the individual couplings J(N,H) and J(H,N) were averaged by a fast intramolecular proton tautomerism between two forms, it is shown that the sum $|J(N,H)+J(H,N)|$ generally represents a measure of the hydrogen-bond strength in a similar way to δ_H and J(N,N). The NMR spectroscopic parameters of $DMANH^+$ and of 4-nitro-$DMANH^+$ are independent of the anion in the case of CD_3CN, which indicates ion-pair dissociation in this solvent. By contrast, studies using CD_2Cl_2, [D_8]toluene as well as the freon mixture CDF_3/CDF_2Cl, which is liquid down to 100 K, revealed an influence of temperature and of the counteranions. Whereas a small counteranion such as trifluoroacetate perturbed the hydrogen bond, the large noncoordinating anion tetrakis[3,5-bis(trifluoromethyl)phenyl]borate $B[\{C_6H_3(CF_3)_2\}_4]^-$ ($BARF^-$), which exhibits a delocalized charge, made the hydrogen bond more symmetric. Lowering the temperature led to a similar symmetrization, an effect that is discussed in terms of solvent ordering at low temperature and differential solvent order/disorder at high temperatures. By contrast, toluene molecules that are ordered around the cation led to typical high-field shifts of the hydrogen-bonded proton as well as of those bound to carbon, an effect that is absent in the case of neutral NHN chelates.

Keywords: counterion interactions · coupling constants · hydrogen bonds · NMR spectroscopy · solvent effects

[a] Dr. M. Pietrzak, J. P. Wehling, S. Kong, Dr. P. M. Tolstoy, Dr. I. G. Shenderovich, Prof. Dr. H.-H. Limbach
Institut für Chemie und Biochemie, Freie Universität Berlin
Takustrasse 3, Berlin (Germany)
Fax: (+49) 30-838-5310
E-mail: limbach@chemie.fu-berlin.de

[b] Dr. C. López, Prof. Dr. R. M. Claramunt
Departamento de Química Orgánica and Bio-Orgánica
Facultad de Ciencias, UNED
Senda del Rey 9, 28040 Madrid (Spain)

[c] Prof. Dr. J. Elguero
Instituto de Química Médica, CSIC
Juan de la Cierva 3, 28006 Madrid (Spain)

[d] Dr. P. M. Tolstoy, Dr. I. G. Shenderovich, Prof. Dr. G. S. Denisov
V. A. Fock Institute of Physics, St. Petersburg University
Ulyanovskaja 1, 198504 Peterhof, St. Petersburg (Russia)

[e] Dr. M. Pietrzak
Institute of Physical Chemistry, Polish Academy of Sciences
Kasprzaka 44/52, 01-224 Warsaw (Poland)

Supporting information for this article is available on the WWW under http://dx.doi.org/10.1002/chem.200902259. It includes a) syntheses of 1-chlorobenzotriazole and 2-chloro-1,3,5-trinitrobenzene (picryl chloride); b) spectra of **10H$^+$** in different solvents; c) tables of ^{1}H chemical shifts and coupling constants of **1**, **10**, and **10H$^+$**; d) indirect determination of coupling constants J(N,N) of NHN hydrogen bonds that are symmetric or that are subject to a degenerate proton tautomerism; and e) a theoretical section showing that the sum of coupling constants $|J(N,H)+J(H,N)|$ of NHN hydrogen bonds are to a good approximation independent of the equilibrium constant of tautomerism.

Introduction

Proton transfer in low-barrier hydrogen bonds is very important in chemistry and biology and represents a challenge for experiment and theory.[1–5] One of the major problems lies in how intermolecular interactions influence the properties of hydrogen bonds. The fate of an asymmetric neutral hydrogen bond AHB in a polar solvent has been firmly established experimentally[6,7] and theoretically.[8,9] Whereas the difference between the isolated and solvated hydrogen bridge at high temperature is small because the solvent molecules are disordered, solvent ordering at low temperatures leads to an increase of the dipole moment of the system (Scheme 1a and b). As a result, the hydrogen atom first

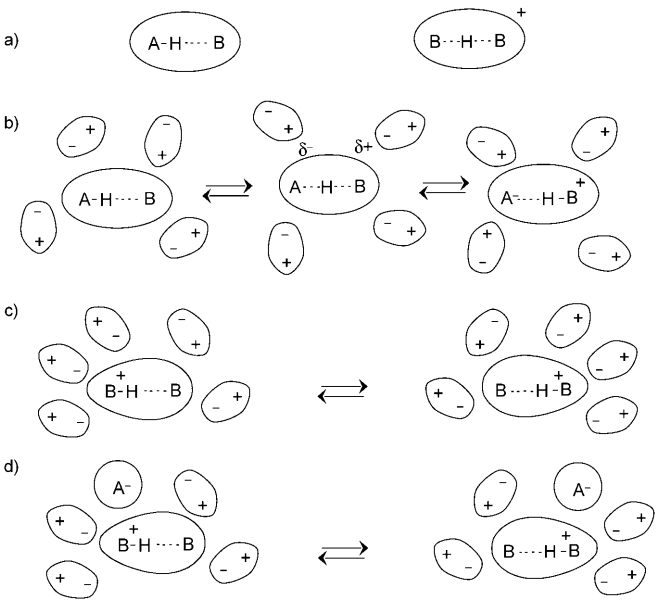

Scheme 1. Scenarios for the influence of intermolecular interactions on hydrogen-bond geometries. a) Asymmetric neutral and symmetric cationic hydrogen bridges in the gas phase. b) Gradual conversion of a neutral hydrogen bridge into a zwitterionic hydrogen bridge induced by ordering of a polar solvent at low temperatures.[6] c) Differential solvent ordering around an ionic hydrogen bridge produces two rapidly interconverting tautomers, also called solvatomers,[11] separated by a solvent barrier. d) Enhanced symmetry breaking by additional interaction with the counterion.

shifts towards the hydrogen-bond center associated with a decrease of the heavy-atom distance, and then forms a zwitterionic species in which the hydrogen bond becomes longer again. By contrast, much less is known about the ionic hydrogen bonds AHA^- or BHB^+. The current opinion is that a symmetric ion in which the hydrogen atom is located in the hydrogen-bond center is strongly perturbed by a polar solvent,[10,11] as illustrated schematically in Scheme 1c, and/or by the counterion (Scheme 1d), which leads to a degenerate tautomerism between two forms. This is because the solvent dipoles as well as ion pairing may favor charge localization and hence proton localization near one or the other heavy atom of the hydrogen bridge as illustrated schematically in Scheme 1. The tautomers produced in this way will be separated by a solvent barrier and interconvert rapidly. They have also been named as "solvatomers".[11] Unfortunately, it is very difficult to obtain information about these interactions using conventional spectroscopic probes.

Therefore, we have used in this study an NMR spectroscopic tool established in the last decade to obtain novel information about the influence of solvation and counterion interactions on cationic hydrogen bonds. It consists of measuring nuclear scalar couplings across hydrogen bonds that contain suitable nuclei with spin $^1/_2$.[12–14]

After their discovery, subsequent model studies showed that couplings across hydrogen bonds provide interesting information about their geometries in solution,[7,15–23] in the solid state,[24,25] as well as in biomolecules.[26–31] In particular, the average position of the proton in a hydrogen bond AH···B can be determined, as J(A,B) exhibits a maximum when the hydrogen atom is located in the hydrogen-bond center. To develop relations between hydrogen-bond geometries and their intrinsic scalar couplings, high-level quantum mechanical calculations have largely contributed.[32–37]

As intermolecular hydrogen bonds can be studied in solution only at low temperatures by NMR spectroscopy,[38] the observation of scalar couplings J(N,N) across intramolecular NHN hydrogen bonds of doubly ^{15}N-labeled 1,8-bis(dimethylamino)naphthalene ($DMANH^+$) at room temperature represented a considerable progress.[39] Prior to this, protonated sponges of the $DMANH^+$ type were studied mainly by a combination of various experimental and theoretical methods and had focused on the question of whether or not the proton moves in a single or double well.[40–43] In solution, such information was obtained by studying the effects of isotopic substitution on NMR spectroscopic chemical shifts.[11,44] Other NMR spectroscopic studies of protonated 1,8-bis(dimethylamino)naphthalenes focused on the determination of the equilibrium constants of tautomerism by analyzing the temperature dependence of the coupling constants J(N,H) and J(H,N).[45–47] The role of the solvent on the hydrogen-bond symmetries of proton sponges was discussed by Perrin et al.[11] in a similar way as visualized in Scheme 1c; the high basicity of DMAN was explained in terms of strain relief upon protonation. However, the coupling constants J(N,N) of protonated sponges have not yet been used as a model for the study of the influence of intermolecular interactions upon the hydrogen-bond symmetries.

To understand how the new tool can be used, let us discuss previous findings of J(N,N) values of systems containing intramolecular NHN hydrogen bonds, which are assembled in Scheme 2. The neutral and anionic seven- and six-membered hydrogen chelates **1**,[17] **2**,[17] **2′**,[18] **3**,[48] and **4**[49] exhibit coupling constants J(N,N) between 8.7 and 16.5 Hz; the positively charged six-membered "protonated proton sponge" 1,8-bis(dimethylamino)naphthalene ($DMANH^+$, $\mathbf{5H^+}$) exhibited only a value of 8.7 Hz.[39] We note that values between 6 and 9 Hz were observed for Watson–Crick nucleic acid base pairs and some higher values up to 10.5 Hz of positively charged Hoogsteen base pairs.[14b] A similar

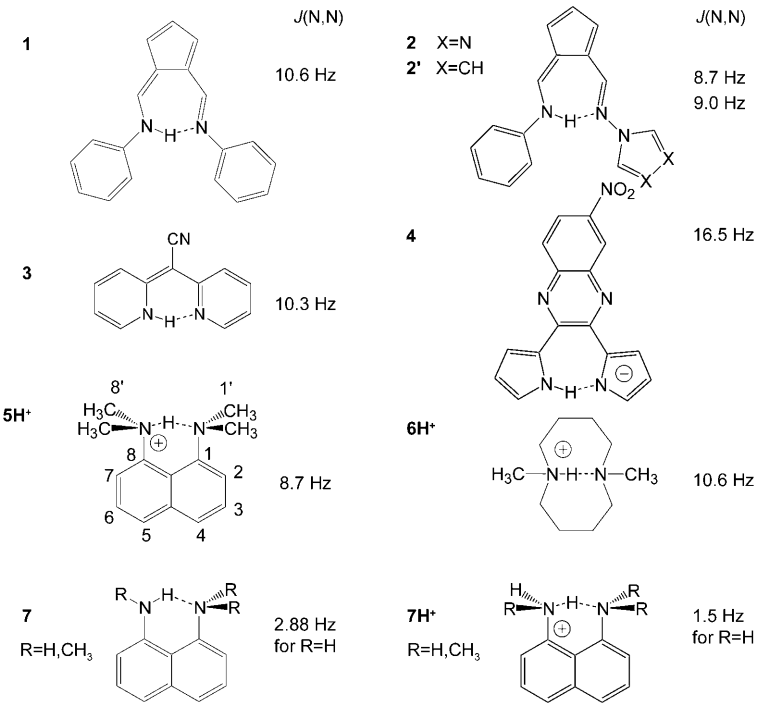

Scheme 2. J(N,N) coupling constants in doubly ^{15}N-labeled hydrogen chelates dissolved in organic solvents: **1**: *N,N′*-diphenyl-6-aminopentafulvene-1-aldimine-$^{15}N_2$.[17] **2**: *N*-phenyl-*N′*-(1,3,4-triazol)-6-aminopentafulvene-1-aldimine-$^{15}N_2$.[16,17] **2′**: *N*-phenyl-*N′*-(pyrrol)-6-aminopentafulvene-1-aldimine-$^{15}N_2$.[18] **3**: bis-(2-pyridyl)-acetonitrile.[48] **4**: 6-nitro-2,3-dipyrrol-2-ylquinoxaline.[49] **5H$^+$**: 1,8-bis(dimethylamino)-naphthalene-H$^+$.[39] **6H$^+$**: 1,6-dimethyl-1,6-diazacyclodecane-H$^+$.[50] **7**: 1,8-bis(amino)-naphthalene.[50] **7H$^+$**: 1,8-bis(amino)-naphthalene-H$^+$ and corresponding analogs, which are singly, doubly and triply methyl substituted at the nitrogen atoms.[50]

value was observed for **6H$^+$**.[50] By contrast, an abnormally small value of 1.5 Hz was observed for protonated 1,8-bis-(amino)naphthalene (DANH$^+$, **7H$^+$**), which increased after successive methylation of the nitrogen atoms. The values observed were even smaller than those of neutral DAN **7**.[50]

As the values of J(N,N) are much less influenced by the tautomerism, we undertook the present study in continuation of our previous work[39] on **5H$^+$** of scalar couplings in the systems listed in Scheme 3. For that purpose, we synthesized the doubly ^{15}N-labeled isotopologues. We varied the substituents and the symmetry of the sponges; the values of J(N,N) of the symmetrically substituted compounds had to be determined indirectly by analysis of the high-order NMR spectroscopic signals of ^{13}C atoms coupled to one of the two ^{15}N nuclei.[48,50] Inspired by the outcome of the experimental results described in this paper, some of us have presented a computational study of coupling constants across NHN hydrogen bonds in the gas phase.[51,52]

In particular, we focused on **5H$^+$** and on **10H$^+$**. For these systems, we used larger counteranions such as CF_3COO^- (A^-) and the noncoordinating tetrakis[3,5-bis(trifluoromethyl)phenyl]borate $B[\{C_6H_3(CF_3)_2\}_4]^-$ ($BARF^-$), which we found to improve the solubility of these sponges in polar solvents such as CD_2Cl_2 and the freon mixture CDF_3/CDF_2Cl. In the case of **10H$^+$**[BARF]$^-$, we could even measure some spectra in the nonpolar [D_8]toluene. In fact, we observed for J(N,N) and the other NMR spectroscopic parameters a strong dependence on temperature and the sample composition. Knowledge of such interactions is important if one wants to compare values computed for the isolated systems with those measured in condensed phases. In the following, we present the results of our measurements, which are then discussed.

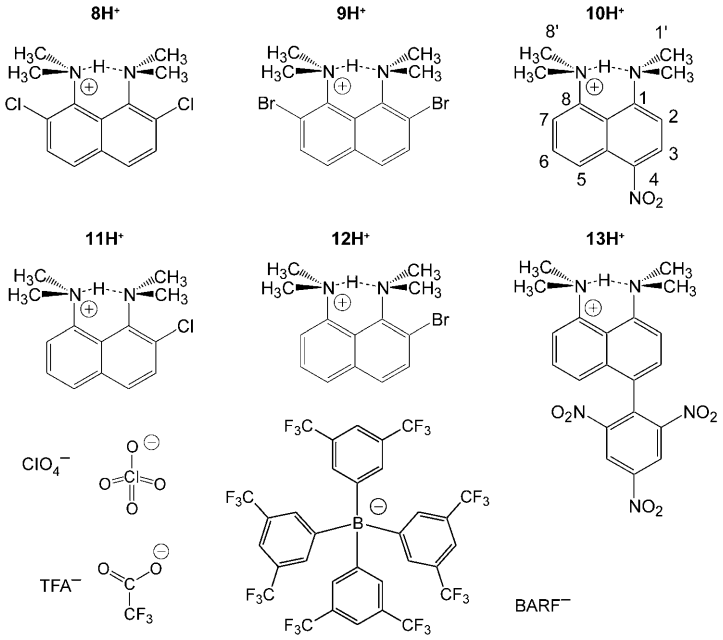

Scheme 3. Doubly ^{15}N-labeled protonated proton sponges for which coupling constants across the intramolecular ^{15}N···H···^{15}N bridges are reported in this study.

Results

NMR spectra: The NMR parameters of all systems measured under different conditions are assembled in Table 1 and in Table S1 of the Supporting Information.

Perchlorate salts of protonated proton sponges in [D_3]acetonitrile: The ^{1}H, ^{15}N, and ^{13}C{^{1}H} NMR spectra of

Table 1. NMR spectroscopic parameters of the intramolecular N–H···N hydrogen bonds of NHN chelates and protonated proton sponges of the DMAN type.

Compound	Ref.	Counterion	Solvent	T [K]	δ_H [ppm]	δ_{NHN} [ppm]	δ_{NHN} [ppm]	J(N,H) [Hz]	J(H,N) [Hz]	J(N,H)+J(H,N) [Hz]	J(N,N) [Hz]
1	[17]	–	$CDCl_3$	293	15.28	–	–	−40.8	−40.8	−81.6	10.6[b]
1	[a]	–	[D_8]toluene	293	15.53	–	–	−41	−41	−82	–
2	[16]	–	$CDCl_3$	293	12.77	–	–	−88.6	+4.4	−84.2	8.7
2′	[18]	–	$CDCl_3$	293	13.26	–	–	−88.2	+4.0	−84.2	9.0
3	[48]	–	$CDCl_3$	293	16.15	–	–	−40.0	−40.0	−80	10.3[b]
4	[49]	$Na^+ \cdot n$DMSO	CD_2Cl_2/[D_6]DMSO (5:1)	193	20.51	–	–	−55.2	−24.7	−79.9	16.5
5H$^+$	[39]	ClO_4^-	CD_3CN	293	18.6	−346.7	−346.7	−30.5	−30.5	−61.0	8.7[b]
5H$^+$	[a]	$BARF^-$	CD_3CN	293	18.69	−347.92	−347.92	−30.57	−30.57	−61.14	–
5H$^+$	[a]	$BARF^-$	CD_3CN	273	18.77	−347.90	−347.90	−30.53	−30.53	−61.05	–
5H$^+$	[a]	$BARF^-$	CD_3CN	253	18.85	−347.88	−347.88	−30.45	−30.45	−60.80	–
5H$^+$	[a]	$BARF^-$	CD_3CN	233	18.92	−347.85	−347.85	−30.38	−30.38	−60.76	–
8H$^+$	[a]	ClO_4^-	CD_3CN	293	20.2	−349.6	−349.6	−27.8	−27.8	−55.6	8.3[b]
9H$^+$	[a]	ClO_4^-	CD_3CN	293	20.2	−349.1	−349.1	−27.6	−27.6	−55.2	8.2[b]
11H$^+$	[a]	ClO_4^-	CD_3CN	293	18.7	−352.6	−345.0	−47.8	−12.1	−59.9	8.16
12H$^+$	[a]	ClO_4^-	CD_3CN	293	18.8	−351.7	−345.0	−50.1	−11.9	−62.0	8.10
13H$^+$	[a]	ClO_4^-	CD_3CN	293	18.8	−347.5	−346.7	−35.0	−25.9	−60.9	8.85
13H$^+$	[46]	ClO_4^-	[D_6]DMSO	293	18.43	−345.2	−344.4	−36.2	−27.9	−64.1	–
10H$^+$	[a]	TFA^-	CD_3CN	293	18.73	−345.9	−345.2	−40.2	−20.3	−60.5	8.80
10H$^+$	[a]	ClO_4^-	CD_3CN	293	18.73	−346.0	−345.3	−40.2	−20.5	−60.7	8.8
10H$^+$	[a]	ClO_4^-	[D_6]acetone	293	19.03	–	–	−39.8	−20.9	−60.7	–
10H$^+$	[a]	$BARF^-$	CD_2Cl_2	293	19.48	−347.0	−346.3	−38.7	−20.0	−58.7	9.27
10H$^+$	[a]	$BARF^-$	CD_2Cl_2	268	19.57	−347.0	−346.3	−39.1	−19.6	−58.7	9.31
10H$^+$	[a]	$BARF^-$	CD_2Cl_2	243	19.67	−346.9	−346.2	−39.5	−19.1	−58.6	9.40
10H$^+$	[a]	$BARF^-$	CD_2Cl_2	218	19.76	−346.9	−346.1	−40.0	−18.6	−58.6	9.48
10H$^+$	[a]	$BARF^-$	CD_2Cl_2	193	19.85	−346.8	−346.0	−40.5	−17.6	−58.1	9.56
10H$^+$	[a]	$BARF^-$	CDF_3/CDF_2Cl (3:1)	297	19.70	–	–	−38.9	−19.8	−58.7	9.26
10H$^+$	[a]	$BARF^-$	CDF_3/CDF_2Cl (3:1)	193	20.21	–	–	−40.1	−17.8	−57.9	9.66
10H$^+$	[a]	$BARF^-$	CDF_3/CDF_2Cl (3:1)	158	20.36	–	–	−40.4	−17.2	−57.6	9.78
10H$^+$	[a]	$BARF^-$	CDF_3/CDF_2Cl (3:1)	130	20.46	–	–	−40.5	−16.9	−57.4	9.87
10H$^+$	[a]	$BARF^-$	[D_8]toluene	294	18.13	−348.3	−349.1	38.8±0.5	21.2±0.5	60.0	9.4±0.5
10H$^+$	[a]	$BARF^-$	[D_8]toluene	273	18.16	–	–	–	–	–	–
10H$^+$	[a]	$BARF^-$	[D_8]toluene	243	18.26	–	–	38.8±0.5	21.2±0.5	60.0	–
10H$^+$	[a]	TFA^-	CD_2Cl_2	293	18.86[c]	–	–	−41.7[c]	−19.2[c]	−60.9[c]	8.64[c]
10H$^+$	[a]	TFA^-	CD_2Cl_2	273	18.99	–	–	−42.0	−18.7	−60.7	8.71
10H$^+$	[a]	TFA^-	CD_2Cl_2	253	19.09	–	–	−42.3	−18.1	−60.4	8.86
10H$^+$	[a]	TFA^-	CD_2Cl_2	233	19.20	–	–	−42.6	−17.6	−60.2	8.98
10H$^+$	[a]	TFA^-	CD_2Cl_2	213	19.32	–	–	−42.8	−17.2	−60.0	9.07
10H$^+$	[a]	TFA^-	CD_2Cl_2	193	19.43	–	–	−43.1	−16.7	−59.8	9.15
10H$^+$	[45]	ClO_4^-	[D_6]DMSO	293	18.40	−344.6	−344.0	−40.4	−21.8	−62.2	–

[a] This work. [b] Indirect detection by means of ^{13}C NMR spectroscopy. [c] Extrapolated from low temperatures. $\delta_{NHN} \equiv \delta_{N8HN1}$, $\delta_{NHN} \equiv \delta_{N8HN1}$, J(N,H) = J(N8,H), J(H,N) = J(H,N1). For the atom numbering see Scheme 2. TFA^-: a mixture of trifluoroacetate A^- and the homoconjugated anion AHA^-.

saturated solutions (between 0.1 and 0.2 M) of **8** to **13** and of the corresponding protonated perchlorates **8H$^+$** to **13H$^+$** in CD_3CN were recorded at room temperature using standard techniques. Typical spectra are included in the Supporting Information. ^1H and ^{15}N chemical shifts and the corresponding absolute one-bond coupling constants $|J(N,H)|$ and $|J(H,N)|$ could be determined directly from the signal splittings in the ^1H and the ^{15}N spectra. These coupling constants are negative because of the negative gyromagnetic ratio of ^{15}N (Table 1). In the case of the unsymmetric ions, the values of J(N,N) were obtained directly from the ^1H decoupled ^{15}N spectra. By contrast, in the case of **8H$^+$** and **9H$^+$**, these values were determined by line-shape analysis of the high-order $^{13}C\{^1H\}$ signals of C1 and of the methyl groups as described previously.[39]

In the case of the symmetrically substituted ions, the equilibrium constants K_{ab} of tautomerism [Eq. (1)] are unity, thus leading to $J(N,H) = J(H,N)$.

$$[N8{-}H\cdots N1] \equiv \mathbf{a} \rightleftharpoons \mathbf{b} \equiv [N8\cdots H{-}N1] \quad (1)$$

By contrast, in the case of the asymmetric ions, H is located preferentially on N8, that is, $K_{ab} < 1$ and $|J(N,H)| > |J(H,N)|$ (see the theoretical section of the Supporting Information). However, to determine K_{ab}, knowledge is needed of the intrinsic coupling constants, which are influenced by temperature-dependent solute–solvent interactions. As this information is lacking, we did not attempt to determine the K_{ab} values.

Variable-temperature and solvent-dependent NMR spectroscopy of ***5H*$^+$ *and* ***10H*$^+$: To gain more insight into the influence of intermolecular interactions, further experiments were performed on $\mathbf{5H}^+$ and on $\mathbf{10H}^+$. In Figure 1a, the

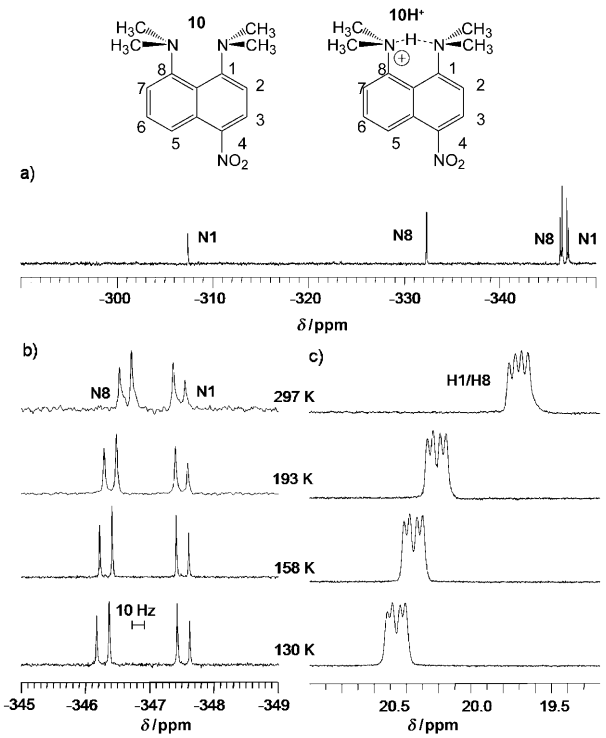

Figure 1. NMR spectra of a solution of **10** (0.02 M) in CDF_3/CDF_2Cl (3:1) in the presence of HBARF (Scheme 3): a) $^{15}N\{^1H\}$ NMR spectrum at 293 K; b) $^{15}N\{^1H\}$ NMR signals of $\mathbf{10H}^+$ at different temperatures; and c) low-field ^1H NMR signal of $\mathbf{10H}^+$ at different temperatures.

temperature-dependent ^{15}N signals N1 and N8 of a solution (0.02 M) of **10** in CDF_3/CDF_2Cl (3:1) are depicted, to which HBARF had been added in a molar ratio of about 80%. This produces predominantly $\mathbf{10H}^+$, which is—even at room temperature—in slow exchange with the residual base **10**. The signal assignment follows those reported in the literature for samples of **10** and $\mathbf{10H}^+$ that contain ^{15}N in natural abundance.[45] We note that the chemical shift difference between N1 and N8 is much larger for **10** as compared to $\mathbf{10H}^+$; moreover, N1 appears at lower field in **10** but at higher field in $\mathbf{10H}^+$.

An expansion of the ^{15}N signals of $\mathbf{10H}^+$ is depicted in Figure 1b for selected temperatures. As ^1H decoupling was employed, typical spectra of an AB spin system are observed, governed by J(N,N). The corresponding signals of the hydrogen-bonded proton are depicted in Figure 1c. They are split by the coupling constants $J(N,H)=J(N8,H)$ and $J(H,N)=J(H,N1)$. These values strongly depend on temperature. The chemical shift is increased substantially when temperature is lowered.

We obtain similar spectra of $\mathbf{10H}^+[BARF]^-$ using CD_2Cl_2 as solvent. In spite of a low solubility, we also were able to obtain ^1H spectra for $[D_8]$toluene; however, efforts to obtain spectra in $[D_8]$toluene using other counterions were not successful. The spectra are depicted in Figure S1 and S2 of the Supporting Information and indicate major solvent effects discussed below. Different NMR spectroscopic parameters were also obtained when trifluoroacetic acid was used to protonate **10** (Figure S3 in the Supporting Information). The ^{15}N signals were similar to those in Figure 1, but line broadening at room temperature indicated a fast proton exchange of $\mathbf{10H}^+$ with some remaining **10**. ^1H NMR spectroscopy showed separate lines for the mobile proton in $\mathbf{10H}^+$, broad at 298 K but giving rise to a similar splitting pattern at lower temperatures as shown in Figure 1. At 298 K, a broad line was observed at $\delta=10.2$ ppm for various trifluoroacetic acid species and residual water. When the temperature was lowered, the latter was precipitated as ice and the remaining trifluoroacetic acid signal broadened and decoalesced below 193 K into a sharp line at $\delta=20$ ppm. This chemical shift is typical for the homoconjugated trifluoroacetate anion AHA^-.[53] A detailed analysis of this signal was, however, beyond the scope of this study.

Discussion

Before we enter the discussion of the results obtained in this study, let us make some general remarks. As illustrated in Scheme 4, it is now accepted that the two hydrogen-bond

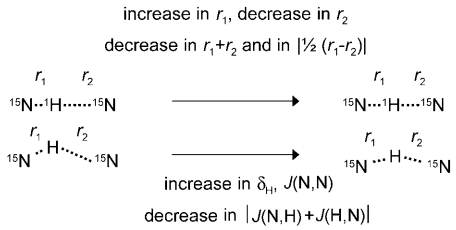

Scheme 4. Geometric hydrogen-bond correlation and its effect on NMR spectroscopic parameters.

distances r_1 and r_2 are correlated with each other in the sense that if r_1 is increased r_2 will be decreased. This means that also the proton coordinate $|q_1|=|\frac{1}{2}(r_1-r_2)|$ and the heavy-atom coordinate $q_2=r_1+r_2$ are correlated. For a linear hydrogen bond, $|q_1|$ represents the distance of the hydrogen atom from the hydrogen-bond center, and q_2 represents the heavy-atom distance. The correlation implies that a compression of the hydrogen bond, that is, a reduction of q_2 leads to a displacement of the hydrogen atom towards the hydrogen-bond center as illustrated in Scheme 4. This process is also addressed as a "strengthening" of the hydrogen bond, or as a "symmetrization", although symmetry is not achieved, rather only a step towards symmetry is taken.

This "symmetrization" leads to an increase of the chemical shift δ_H of the hydrogen-bonded proton—that is, a low-

field shift—and in the case of NHN hydrogen bonds, to an increase of the coupling constant J(N,N). Later we will show that also the sum $|J(\mathrm{N,H})+J(\mathrm{H,N})|$ represents a measure of the hydrogen-bond geometry. Various effects change the hydrogen-bond properties, namely, chemical substitution, counteranion, solvent, and temperature. In the following, we will discuss these findings in more detail.

NMR spectroscopic parameters: As an overview, in Figure 2 are plotted the room-temperature coupling constants J(N,N) and sums $|J(\mathrm{N,H})+J(\mathrm{H,N})|$ of the different systems as a

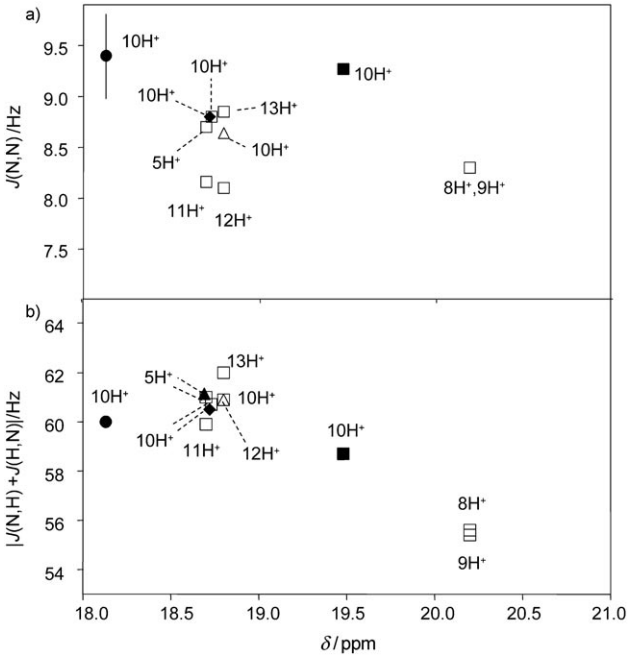

Figure 2. Room-temperature coupling constants a) J(N,N) and b) $|J(\mathrm{N,H})+J(\mathrm{H,N})| \equiv -[J(^{15}\mathrm{N},^{1}\mathrm{H})+J(^{1}\mathrm{H},^{15}\mathrm{N})]$ of $^{15}\mathrm{N}^{1}\mathrm{H}^{15}\mathrm{N}$ hydrogen bonds of various protonated proton sponges of the 1,8-bis(dimethylamino)naphthalene-H^+ type (▲: $BARF^-$, CD_3CN; ■: $BARF^-$, CD_2Cl_2; ●: $BARF^-$, $[D_8]$toluene; ◆: TFA^-, CD_3CN; △: TFA^-, CD_2Cl_2; □: ClO_4^-, CD_3CN; see Schemes 2 and 3) as a function of the chemical shift δ_H of the hydrogen-bonded proton.

function of the chemical shifts (δ_H) of the hydrogen-bonded protons. Surprisingly, the NMR spectroscopic parameters of $\mathbf{5H^+}$ and of all asymmetric ions are similar. As compared to the asymmetric ions $\mathbf{11H^+}$ and $\mathbf{12H^+}$, the symmetric ions $\mathbf{8H^+}$ and $\mathbf{9H^+}$ exhibit larger values of δ_H and of J(N,N), and lower values of $|J(\mathrm{N,H})+J(\mathrm{H,N})|$, which indicates a strengthening of the hydrogen bond according to Scheme 4. However, the influence of solvent and counteranion is of the same order or even larger than the influence of chemical substitution, and it is difficult to distinguish the different effects solely on the basis of the room-temperature data of Figure 2.

For $\mathbf{5H^+}$ and $\mathbf{10H^+}$ we were able to obtain additional information by low-temperature NMR spectroscopy. Their NMR spectroscopic parameters are very similar. As the determination of J(N,N) was more difficult for $\mathbf{5H^+}$ than for $\mathbf{10H^+}$, we studied the latter system in more detail. In Figure 3 are plotted their chemical shifts (δ_H) and in Figure 4 the coupling constants J(N,N) as a function of temperature.

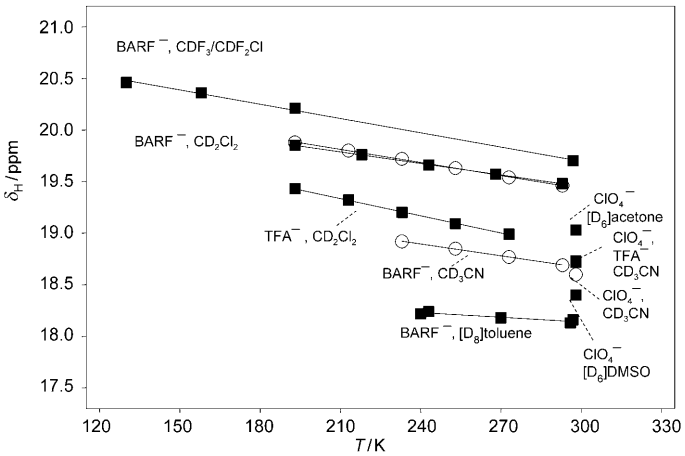

Figure 3. Chemical shift δ_H of the hydrogen-bonded proton of $\mathbf{5H^+}$ (○) and of $\mathbf{10H^+}$ (■) measured under different conditions as a function of temperature.

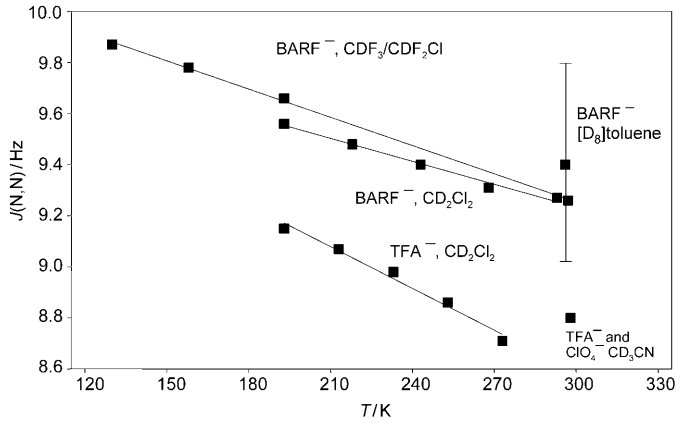

Figure 4. Coupling constant J(N,N) of $\mathbf{10H^+}$ measured under different conditions as a function of temperature.

The first result to note is that the values of δ_H are independent of the anion if CD_3CN is used as solvent. This provides evidence that in acetonitrile the ion pairs are dissociated because of the large dielectric constant. By contrast, for the less polar solvents CD_2Cl_2 and CDF_3/CDF_2Cl, we find that δ_H and J(N,N) are substantially larger for $BARF^-$ relative to trifluoroacetate (TFA^-), which indicates the formation of contact ion pairs in CD_2Cl_2 and CDF_3/CDF_2Cl, and especially in $[D_8]$toluene. We note that Bernatowicz et al.[54] interpreted their longitudinal relaxation time data of **5** and $\mathbf{5H^+}[NO_3]^-$ in $[D_7]$DMF also in terms of ion pairing.

The second main feature of Figures 3 and 4 is that δ_H and J(N,N) are substantially increased upon lowering temperature in all polar solvents, but not in nonpolar $[D_8]$toluene.

The largest values of $\delta = 20.4$ ppm and $J(\mathrm{N,N}) = 9.9$ Hz are reached for CDF_3/CDF_2Cl at 130 K and $BARF^-$ as counteranion. Unfortunately, solubility problems did not allow us to reach lower temperatures; it seems that the values would still increase if temperature could be further lowered. The observed temperature dependence must be associated with the increase of the dielectric constants of the polar solvents when temperature is lowered.[7,22c,55]

These findings are corroborated by the coupling-constant sums $|J(\mathrm{N,H}) + J(\mathrm{H,N})|$, which are plotted in the upper part of Figure 5 as a function of δ_H. We observe a monotonous

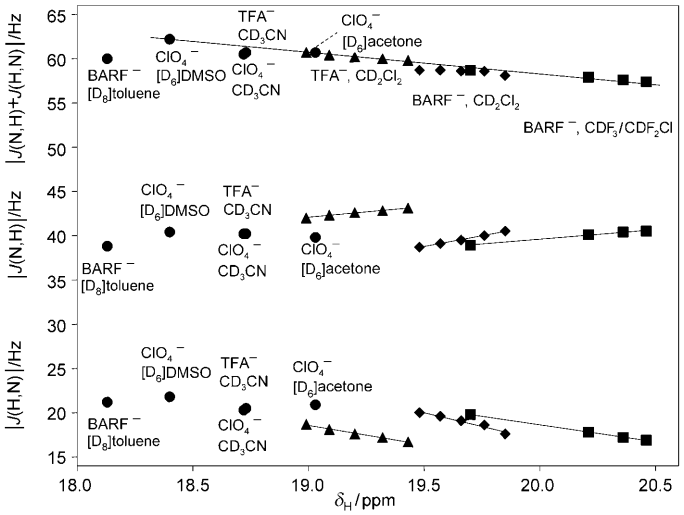

Figure 5. Coupling constants $|J(\mathrm{N,H}) + J(\mathrm{H,N})|$, $|J(\mathrm{N,H})|$, and $|J(\mathrm{H,N})|$ of the NHN hydrogen bonds of $\mathbf{10H^+}$ measured under different conditions as a function of the chemical shift δ_H of the hydrogen-bonded proton.

decrease of $|J(\mathrm{N,H}) + J(\mathrm{H,N})|$ with increasing value of δ_H, and hence with increasing values of $J(\mathrm{N,N})$. With the exception of the value for $[D_8]$toluene, all data points—even if they were derived under different conditions—are located on the same correlation line. To shift the data point of $[D_8]$toluene to the correlation line, a low-field shift of about $\delta = 1$ ppm is required.

By contrast, the temperature dependence of the individual coupling constants $J(\mathrm{N,H})$ and $J(\mathrm{H,N})$ depicted in the lower part of Figure 5 is more complex and will be discussed later.

The case of the ion pair $\mathbf{10H^+}[\mathrm{BARF}]^-$ in $[D_8]$toluene requires some special discussion. A closer look at the chemical shifts of the aromatic and methyl protons of $\mathbf{10H^+}$ (Table S1 in the Supporting Information) indicates that in addition to the observed high-field shift of the mobile proton, the aromatic and methyl proton signals also exhibit such a shift, although to a smaller extent. For comparison, we have re-measured the chemical shifts of the neutral chelate **1** (Scheme 2) in $CDCl_3$ and in $[D_8]$toluene. The hydrogen-bond proton as well as the CH protons do not show any substantial difference in both solvents. Therefore, it seems that toluene is already highly ordered around $\mathbf{10H^+}$ at room temperature. This finding can be explained in terms of the high polarizability of this solvent, which is revealed by very large negative entropies of ion-pair formation.[56] In the case of $\mathbf{10H^+}[\mathrm{BARF}]^-$, the arrangement of the solvent molecules must be such that the ring currents induced by the aromatic toluene ring lead to the observed high-field shifts of $\mathbf{10H^+}$. In principle, using appropriate quantum mechanical calculations, it could be possible to obtain information about how the solvent shell is arranged around the ion pair, and whether a single molecule is located between both ions.

Solvent ordering and ion pairing: The scenarios in Scheme 5 offer a qualitative explanation for the findings depicted in Figures 3–5. Scheme 5a deals with the case of the dissociated

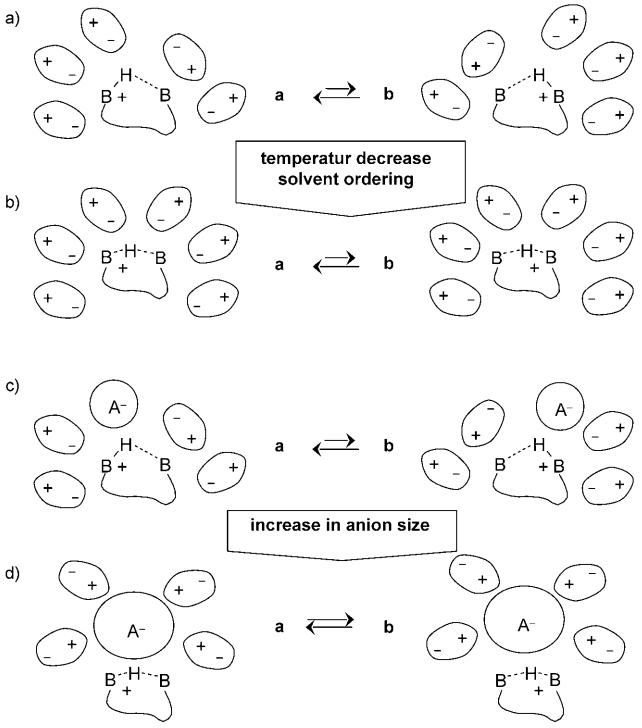

Scheme 5. a) Differential solvation of a homoconjugated cation at room temperature. The positively charged acceptor site that contains the proton experiences a higher local solvent order than the neutral acceptor site. Tautomerism is accompanied by solvent reorganization. b) Solvent ordering by lowering the temperature increases the symmetry of the hydrogen bond. c) Interaction with a small counteranion that is placed in an asymmetric way with respect to the hydrogen bond weakens the hydrogen bond. d) Interaction with a large counteranion in which the charge is well shielded and that is placed in a symmetric way with respect to the hydrogen bond can symmetrize and strengthen the hydrogen bond.

ion pair as found for acetonitrile. At room temperature, the solvent molecules around the positively charged nitrogen atom may exhibit a higher local-order parameter than those in the vicinity of the neutral nitrogen atom. This can weaken the hydrogen bond through ion–dipole interactions in both tautomers **a** and **b**. When the temperature is lowered

and solvent ordering occurs, the hydrogen bond becomes more symmetric (Scheme 5b). This "symmetrization" leads to an increase of δ_H, of J(N,N), and to a decrease of the sum $|J(N,H)+J(H,N)|$. By contrast, lowering the temperature also leads to a decrease of the equilibrium constant of tautomerism K_{ab} and hence to an increase of the difference $|J(N,H)-J(H,N)|$. Both trends are illustrated in Figure 5.

Scheme 5 also illustrates the role of the counteranion, which now forms a contact or solvent-separated ion pair with the cation that contains an intramolecular hydrogen bond. When the anion is small (Scheme 5c), it will again perturb the hydrogen bond symmetry and weaken it if it is placed asymmetrically.[57] By contrast, a large counteranion in which the negative charge is well shielded and delocalized[58] will lead to a symmetrization, that is, strengthening of the hydrogen bond as depicted schematically in Scheme 5d. Solvent reorganization at low temperatures will still play an important role.

The scenarios of Scheme 5 might also explain the results of Lloyd-Jones et al.,[50] who found particularly small values of J(N,N) for solutions of iodides of partially methylated protonated proton sponges in acetonitrile. Successive replacement of methyl by hydrogen reduced the values of J(N,N). Thus only 1.5 Hz were observed for $\mathbf{7H^+}$ (Scheme 2, R = H). Unfortunately, because of the fast NH_3 group rotation and fast proton exchange, the chemical shift values of the hydrogen-bonded protons could not be determined. On the other hand, DFT calculations showed that the NHN hydrogen-bond geometries did not substantially change when the methyl groups were replaced by hydrogen.[50] These small values can be interpreted in terms of microsolvation of the NH groups by solvent molecules, which lowers the hydrogen-bond symmetry. This is essentially the case of Scheme 5a.

Effects of chemical structure: Finally, we compare in Figure 6 the values of $|J(N,H)+J(H,N)|$ as well as those of J(N,N) for $\mathbf{10H^+}$ as a function of δ_H with those obtained before from the NHN chelates **1** to **4** (Scheme 2). For both types of compounds, we note a more or less linear decrease of $|J(N,H)+J(H,N)|$ and an increase of J(N,N) when the chemical shift is increased.

For intrinsic couplings it has been well established experimentally that they increase with an increasing s character of the hybridization of nitrogen.[59] These trends have been confirmed by theoretical DFT calculations.[15,32] Thus, sp^3 nitrogen atoms exhibit typical couplings around −75 Hz and sp^2 nitrogen atoms around −90 Hz in which the s character is 33%. Pyrroles exhibit values of about −100 Hz from which an s character of about 36% has been derived.[59] It is thus clear that the sum $|J(N,H)+J(H,N)|$ is smaller for $\mathbf{10H^+}$ than for the NHN chelates (Figure 6). As **4** is of the pyrrole type, its value might be larger than predicted by the line connecting the other chelates **1** to **3**. Noteworthy is the finding of maximum chemical shifts around $\delta_H = 20.5$ ppm both for the NHN chelate **4** as well as for the protonated sponge $\mathbf{10H^+}$. Normally, one would expect similar hydrogen-bond distances r_1 and r_2 in both cases. However, the coupling-constant sum $|J(N,H)+J(H,N)|$ as well as the coupling constants J(N,N) are substantially smaller for the protonated sponge relative to the NHN chelates. The maximum value of J(N,N) observed for $\mathbf{10H^+}$ is 9.9 Hz, whereas the anion **4** exhibits a value of 16.5 Hz, which is the largest value for NHN hydrogen bonds that have been reported up to date.[49] Here, the countercation was Na^+ solvated by several [D$_6$]DMSO molecules. Hence, **4** represented a solvent-separated ion pair in which the effects of cation–anion interactions were minimized.

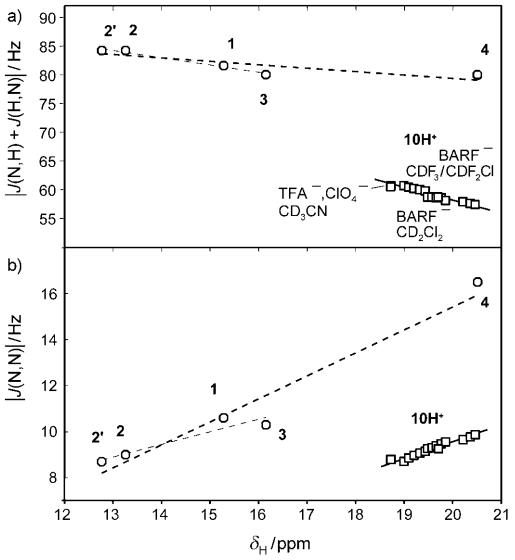

Figure 6. Coupling constants a) $|J(N,H)+J(H,N)|$ and b) J(N,N) of the NHN chelates **1** to **4** (Scheme 2) and of $\mathbf{10H^+}$ measured under different conditions as a function of the chemical shift δ_H of the hydrogen-bonded proton.

The question of whether or not there is a dependence of J(N,N) upon hybridization is less straightforward to answer. Recent high-level calculations by some of us have shown that all coupling constants depend on the hybridization of both N atoms including pyrrole-type and on the charge (neutrals (as **1**, **2**, **3**, **7**), anions (as **4**), and cations (as $\mathbf{5H^+}$–$\mathbf{13H^+}$)).[52] However, J(N,N) also decreases when the hydrogen bond deviates from linearity. Moreover, recent calculations on the protonated HCN dimer indicate a reduction of J(N,N) when the angle between the nitrogen lone pair and the N···H distance vector is not zero.[51] Such a mismatch could be introduced in proton sponges of the $DMANH^+$ type by bulky substituents in the 2-position of the naphthalene ring.

At this point we come back to the influence of the substitution pattern on the NMR spectroscopic parameters of proton sponges. In Figure 5 we showed that the coupling-constant sum $|J(N,H)+J(H,N)|$ decreases monotonously as the proton chemical shift δ_H is increased. We would have then also expected an increase of J(N,N), which was, however, not the case. The reduction of the sum $|J(N,H)+J(H,N)|$ was especially strong for the 2,7-dichloro- and di-

bromo-substituted ions $\mathbf{8H^+}$ and $\mathbf{9H^+}$ (Scheme 3). The unusually high-field-shifted signals of ^{15}N nuclei next to the bulky Cl or Br substituents in nonprotonated forms **8** and **9** (see the Supporting Information) are another manifestation of structural constraint in these molecules. On the other hand, the sum $|J(N,H)+J(H,N)|$ is not reduced in the 2-mono-substituted ions $\mathbf{11H^+}$ and $\mathbf{12H^+}$, in which H is located preferentially on N8 (Table 1), that is, the 2-substituents are located near the lone pair and steric repulsion including angle mismatch should be operative. Therefore, although for a given compound such as $\mathbf{10H^+}$, temperature, solvent, and counteranion dependences of the three spectroscopic probes—δ_H, $J(N,N)$, and $|J(N,H)+J(H,N)|$—are understood in a qualitative way, we have to leave the question open as to why these parameters do not point in the same direction for the cases of $\mathbf{8H^+}$ and $\mathbf{9H^+}$. To solve that question, further experimental and computational studies are necessary.

Finally, we note that 2,7-symmetrically substituted proton sponges, in particular $\mathbf{8H^+}$[40] and $\mathbf{9H^+}$,[41] are known to exhibit unusual hydrogen-bond geometries and vibrations. However, it is difficult at present to establish a connection with the NMR spectroscopic parameters found in this study.

Conclusion

We have arrived at the following conclusions after this study.

1) $|J(N,H)+J(H,N)|$ as a spectroscopic probe: We have shown that not only the ^1H chemical shifts δ_H and coupling constants $J(N,N)$ across NHN hydrogen bonds are measures of the hydrogen-bond strength, but also the coupling-constant sum $|J(N,H)+J(H,N)|$, independent of the presence of a tautomeric equilibrium. Occasionally all three quantities point in the same direction and hence reveal together additional information about a thus far unrecognized problem.
2) Dependence of $J(N,N)$ upon hybridization: Positively charged intramolecular NHN hydrogen bonds of the sp^3 type exhibit smaller coupling constants $J(N,N)$ relative to neutral or anionic hydrogen chelates that contain nitrogen atoms of the sp^2 type, although the ^1H chemical shifts are similar. This finding will require additional computational studies that are similar to those presented previously.[51,52]
3) Intermolecular interactions: We have shown that the NMR spectroscopic parameters of protonated sponges depend strongly on intermolecular interactions. This makes a comparison with calculated values difficult. On the other hand, it provides an interesting molecular probe for local intermolecular interactions. For example, we have verified ion-pair dissociation in the case of the protonated 1,8-bis(dimethylamino)naphthalene cations $\mathbf{5H^+}$ and $\mathbf{10H^+}$ in acetonitrile at room temperature, as no counterion influence on the NMR spectroscopic parameters of the cations was observed. By contrast, contact ion pairs or solvent-separated ion pairs are formed in less polar solvent as reflected in anion-dependent NMR spectroscopic parameters of $\mathbf{5H^+}$ and $\mathbf{10H^+}$. The interaction of such an ion pair with an aromatic solvent such as toluene can lead to high-field shifts of the hydrogen-bonded proton. In such cases one has to rely on $J(N,N)$ and $|J(N,H)+J(H,N)|$ as spectroscopic probes for hydrogen-bond geometries.
4) Symmetrization of cationic hydrogen bonds by ion pairing and solvation: The most important finding of this study is, however, the following. In contrast to our expectations, the NMR spectroscopic parameters of $\mathbf{5H^+}$ and $\mathbf{10H^+}$ indicated a symmetrization of the NHN hydrogen bonds when the temperature was lowered. Two phenomena contribute to this effect: 1) Solvent ordering around the free cations in acetonitrile and around the ion pairs in other less polar solvents. 2) Increase of the size of the counteranion and increased charge delocalization in the latter. We think that these effects are worthy of further experimental and theoretical study in the future.

Experimental Section

General synthesis of doubly ^{15}N-labeled compounds: All unlabeled materials were commercial products purchased from Aldrich, Germany. Potassium [^{15}N]nitrate (95% ^{15}N) was obtained from Chemotrade, Germany. Solvents used for the syntheses were purified using literature procedures.[60] Chloroform was additionally purified over a column with basic aluminum oxide to remove traces of hydrochloric acid. The purification of the products was achieved by column chromatography on neutral aluminum oxide (Brockmann I, 70–230 mesh, $d=2$ cm, $h=20$ cm) from Machery-Nagel, Germany. All reactions were monitored by TLC on neutral aluminum oxide 60 F_{254} (type E), from Merck, Germany, using the same eluent as for column chromatography. The purity of reactants and products was checked by NMR spectroscopy and MS analyses.

Compound $[^{15}N_2]$5: This compound was synthesized as described previously[39,61] by subsequent nitration of naphthalene with [^{15}N]nitric acid, reduction to $[^{15}N_2]$**7**, and permethylation with dimethyl sulfate.

Compound $[^{15}N_2]$8: This compound was prepared by a modification of the synthesis described for the unlabeled compound.[62] A solution of 1-chlorobenzotriazole (see the Supporting Information)[63] (360 mg, 2.34 mmol) in chloroform (20 mL) was added dropwise under stirring to a solution of $[^{15}N_2]$**5** (250 mg, 1.17 mmol) in chloroform (10 mL) cooled to −50 °C. After complete addition, the reaction mass was stirred for an additional 30 min. The solution was concentrated (≈2 mL) and subjected to chromatography. The yellow fraction ($R_f=0.73$) was collected, the solvent was distilled off, and the residue was recrystallized from methanol, thus yielding **8** (320 mg, 96%) as lemon yellow needles. M.p. 48–50 °C.

Compound $[^{15}N_2]$9: This compound was prepared by a modification of the synthesis described for the unlabeled compound.[64] A solution of *N*-bromosuccinimide (280 mg, 1.6 mmol) in chloroform (20 mL) was slowly (≈30 min) added dropwise under stirring to a solution of $[^{15}N_2]$**5** (165 mg, 0.75 mmol) in chloroform (8 mL) cooled to −50 °C. The yellow-brown reaction mass was stirred at −25 °C for an additional 20 min, then the solvent was evaporated. The residue was extracted with hexane (4× 15 mL). Removal of the solvent and recrystallization from methanol yielded **9** (165 mg, 59%) as yellow needles. M.p. 75–76 °C.

Compound [$^{15}N_2$]10: This compound was prepared by a modification of the synthesis described for the unlabeled compound.[65] Compound [$^{15}N_2$]**5** (195 mg, 0.9 mmol) was dissolved in concentrated sulfuric acid (0.9 mL, 96%) and cooled to −15°C. A mixture of concentrated nitric acid (56.7 mg, 100%) and sulfuric acid (0.18 mL, 96%) was added dropwise to the cold solution. After stirring for 5 min, the reaction mixture was poured on ice (20 g) and was neutralized with aqueous ammonia. The precipitate was filtered out and subjected to chromatography (eluent hexane/ethyl acetate 1:1). The fractions containing the product were collected and the solvent was removed under vacuum. The residue was recrystallized from methanol to give **10** (159 mg, 68%) as dark red crystals. M.p. 135–136°C.

Compound [$^{15}N_2$]11: This compound was prepared by a modification of the synthesis described for the unlabeled compound.[62] A solution of 1-chlorobenzotriazole (180 mg, 1.17 mmol) in chloroform (10 mL) was added dropwise under stirring to a solution of [$^{15}N_2$]**5** (250 mg, 1.17 mmol) in chloroform (10 mL) cooled to −15°C. After complete addition, the reaction mass was stirred for another 30 min. The solution was concentrated (≈2 mL) and subjected to chromatography. The yellow fraction (R_f=0.73) was collected and the solvent was distilled, thus yielding **11** (250 mg, 86%) as a pale yellow oil.

Compound [$^{15}N_2$]12: This compound was prepared by a modification of the synthesis described for the unlabeled compound.[64] A solution of *N*-bromosuccinimide (140 mg, 0.8 mmol) in chloroform (10 mL) was slowly (≈30 min) added dropwise under stirring to a solution of [$^{15}N_2$]**5** (165 mg, 0.75 mmol) in chloroform (8 mL) cooled to −20°C. The brown reaction mass was stirred at −15°C for an additional 20 min, concentrated to a volume of 2 mL, and subjected to chromatography (eluent chloroform). The light yellow fraction was collected and the solvent was distilled to yield **12**.

Compound [$^{15}N_2$]13: The synthesis of the unlabeled compound has been described previously.[66] The labeled compound was prepared using the following modified procedure.[67] A solution of 2-chloro-1,3,5-trinitrobenzene in acetonitrile (5 mL; for synthesis, see the Supporting Information) was added under occasional shaking to a solution of [$^{15}N_2$]**5** (108 mg, 0.5 mmol) in acetonitrile (5 mL). After 15 min, water (20 mL) was added, and the solution was extracted with diethyl ether (7×10 mL). The combined extracts were washed with a saturated sodium bicarbonate solution and with water. The ethereal solution was dried over magnesium sulfate and distilled. The residue was recrystallized from acetonitrile to yield **13** (127 mg, 60%) as dark violet crystals.

Protonation of proton sponges: To prepare the protonated perchlorates, a solution of the corresponding base in ethyl acetate (0.04 mmol in 2 mL) was added to perchloric acid (60%, 0.1 mmol). After 2 min, the mixture was diluted with diethyl ether (3 mL). The precipitate was collected, washed with diethyl ether, and dried. Recrystallization from ethanol afforded colorless crystals of the perchlorates. The yields were nearly quantitative.

To prepare the protonated trifluoroacetate **10H$^+$**, trifluoroacetic acid (99%, Aldrich) was added directly to an NMR spectroscopy sample tube that contained the corresponding base dissolved in a deuterated solvent.

To prepare **10H$^+$**[BARF]$^-$, we proceeded as follows. Firstly, a synthesis of HBARF was performed according to the procedure reported by Brookhart et al.[68] and modified by Gründemann.[69] As HBARF is very hygroscopic and sensitive to oxygen, the whole preparation procedure was carried out either in a dry box under an argon atmosphere or on a vacuum line. Proton sponge **10** (0.01 mmol) was placed in an NMR spectroscopy sample tube. HBARF was dissolved in purified and dried dichloromethane. The solution that contained HBARF (about 0.008 mmol) was added directly to the NMR spectroscopy sample tube. Afterwards, the solvent was evaporated on a vacuum line, then CD_2Cl_2 or freon mixture (0.4 mL) was condensed directly in the sample tube.

Samples of **10H$^+$**[BARF]$^-$ in [D_8]toluene were prepared in a different way. The sodium salt of HBARF, NaBARF, which is stable in air under normal conditions, was added to the flask containing water (the solubility of NaBARF in H_2O is very low, so it was not dissolved). Subsequently, a stoichiometric amount of proton sponge **10** and HCl (1.5 equiv) were added, and the solution was stirred at room temperature for approximately 2 d. The nonsoluble product **10H$^+$**[BARF]$^-$ was then filtered and dried under vacuum for another day. Then the weighted amount of the substance was placed into the NMR spectroscopic sample tube and the solvent, [D_8]toluene, was added by means of vacuum transfer. Prior to that, [D_8]toluene was dried over fresh molecular sieves and basic Al_2O_3.

Synthesis of the deuterated freon mixture CDF_3/CDF_2Cl: A modification of the procedure reported by Golubev et al. was used.[70] SbF_3 (30 g, 168 mmol), $CDCl_3$ (20 g, 168 mmol), and $SbCl_5$ (1.5 mL) were mixed inside a Teflon-coated autoclave and heated to 100°C for a few hours. After the pressure had risen to 30–35 bar, heating was continued for another hour. Afterwards, the autoclave was cooled to room temperature, and the freon mixture was condensed through a small column filled with KOH to a bulb filled with KOH on the high-vacuum line (10^{-6} mbar). During this process it was degassed several times to remove air in the system. The freon mixture was then carefully thawed to a temperature of −50°C, at which it was left for 45 min. The freon mixture was condensed into a small steel lecture bottle filled with some dry tetrabutylammonium fluoride, in which it was left overnight. The next day it could be condensed to another steel lecture bottle for long-term storage. It was dried for 30 min with Al_2O_3 directly prior to use. The CDF_3/CDF_2Cl ratio was 3:1 as determined from the residual solvent ^{1}H NMR spectroscopic signals.[7]

NMR spectroscopy experiments: The NMR spectroscopy measurements were carried out using a Bruker AMX 500 instrument operating at 500.13 MHz for ^{1}H, at 125.76 MHz for ^{13}C, and at 50.70 MHz for ^{15}N. A Bruker AC 250 spectrometer operating at 250.13 MHz for ^{1}H and at 62.90 MHz for ^{13}C and a Bruker DRX 750 spectrometer operating at 749.98 MHz for ^{1}H and at 188.58 MHz for ^{13}C were used for the measurements at other magnetic fields. ^{1}H and ^{13}C chemical shifts are given versus TMS, and ^{15}N chemical shifts versus external nitromethane. For the NMR spectroscopy experiments using CDF_3/CDF_2Cl as solvent, special thick-wall NMR spectroscopy tubes (Wilmad, Buena) were employed, equipped with a Teflon-needle valve.

Acknowledgements

This work has been supported by the Deutsche Forschungsgemeinschaft and the Fonds der Chemischen Industrie (Frankfurt).

[1] *Hydrogen Transfer Reactions, Vols. 1–4*, Wiley-VCH, Weinheim, **2007**.
[2] H. H. Limbach, *Hydrogen Transfer Reactions* (Eds.: J. T. Hynes, J. Klinman, H. H. Limbach, R. L. Schowen), **2007**, Chapter 6, pp. 135–221.
[3] a) H. H. Limbach, J. Manz, *Ber. Bunsenges. Phys. Chem.* **1998**, *102*, 289–291; b) K. B. Schowen, H. H. Limbach, G. S. Denisov, R. L. Schowen, *Biochim. Biophys. Acta* **2000**, *1458*, 43–62.
[4] *Isotope Effects in the Biological and Chemical Sciences* (Eds.: A. Kohen, H. H. Limbach), Taylor & Francis, Boca Raton FL, **2005**.
[5] H. H. Limbach, J. M. Lopez, A. Kohen, *Phil. Trans. B* **2006**, *361*, 1399–1415.
[6] N. S. Golubev, G. S. Denisov, S. N. Smirnov, D. N. Shchepkin, H. H. Limbach, *Z. Phys. Chem. (Muenchen Ger.)* **1996**, *196*, 73–84.
[7] I. G. Shenderovich, A. P. Burtsev, G. S. Denisov, N. S. Golubev, H. H. Limbach, *Magn. Reson. Chem.* **2001**, *39*, S91-S99.
[8] M. Ramos, I. Alkorta, J. Elguero, N. S. Golubev, G. S. Denisov, H. Benedict, H. H. Limbach, *J. Phys. Chem. A* **1997**, *101*, 9791–9800.
[9] P. M. Kiefer, J. T. Hynes, *Isr. J. Chem.* **2004**, *44*, 171–184.
[10] A. Warshel, A. Papazyan, P. A. Kollman, *Science* **1995**, *269*, 102–104.
[11] a) C. L. Perrin, B. K. Ohta, *J. Mol. Struct.* **2001**, *559–601*, 1–12; b) C. L. Perrin, J. S. Lau, *J. Am. Chem. Soc.* **2006**, *128*, 11820–11824; c) C. L. Perrin, J. S. Lau, B. K. Ohta, *Pol. J. Chem.* **2003**, *77*, 1693–1702.

[12] I. G. Shenderovich, S. N. Smirnov, G. S. Denisov, V. A. Gindin, N. S. Golubev, A. Dunger, R. Reibke, S. Kirpekar, O. L. Malkina, H. H. Limbach, *Ber. Bunsenges. Phys. Chem.* **1998**, *102*, 422–428.
[13] N. S. Golubev, I. G. Shenderovich, S. N. Smirnov, G. S. Denisov, H. H. Limbach, *Chem. Eur. J.* **1999**, *5*, 492–497.
[14] A. J. Dingley, S. Grzesiek, *J. Am. Chem. Soc.* **1998**, *120*, 8293–8297.
[15] H. Benedict, I. G. Shenderovich, O. L. Malkina, V. G. Malkin, G. S. Denisov, N. S. Golubev, H. H. Limbach, *J. Am. Chem. Soc.* **2000**, *122*, 1979–1988.
[16] R. M. Claramunt, D. Sanz, S. H. Alarcón, M. Pérez-Torralba, J. Elguero, C. Foces-Foces, M. Pietrzak, U. Langer, H. H. Limbach, *Angew. Chem.* **2001**, *113*, 434–437; *Angew. Chem. Int. Ed. Engl.* **2001**, *40*, 420–423.
[17] M. Pietrzak, H. H. Limbach, M. Pérez-Torralba, D. Sanz, R. M. Claramunt, J. Elguero, *Magn. Reson. Chem.* **2001**, *39*, S100-S108.
[18] D. Sanz, M. Pérez-Torralba, S. H. Alarcón, R. M. Claramunt, C. Foces-Foces, J. Elguero, *J. Org. Chem.* **2002**, *67*, 1462–1471.
[19] I. G. Shenderovich, P. M. Tolstoy, N. S. Golubev, S. N. Smirnov, G. S. Denisov, H. H. Limbach, *J. Am. Chem. Soc.* **2003**, *125*, 11710–11720.
[20] I. G. Shenderovich, H. H. Limbach, S. N. Smirnov, P. M. Tolstoy, G. S. Denisov, N. S. Golubev, *Phys. Chem. Chem. Phys.* **2002**, *4*, 5488–5497.
[21] a) A. J. Dingley, J. E. Masse, R. D. Peterson, M. Barfield, J. Feigon, S. Grzesiek, *J. Am. Chem. Soc.* **1999**, *121*, 6019–6027; b) M. Barfield, A. J. Dingley, J. Feigon, S. Grzesiek, *J. Am. Chem. Soc.* **2001**, *123*, 4014–4022.
[22] a) S. N. Smirnov, N. S. Golubev, G. S. Denisov, H. Benedict, P. Schah-Mohammedi, H. H. Limbach, *J. Am. Chem. Soc.* **1996**, *118*, 4094–4101; b) H. H. Limbach, M. Pietrzak, S. Sharif, P. M. Tolstoy, I. G. Shenderovich, S. N. Smirnov, N. S. Golubev, G. S. Denisov, *Chem. Eur. J.* **2004**, *10*, 5195–5204; c) S. N. Smirnov, H. Benedict, N. S. Golubev, G. S. Denisov, M. M. Kreevoy, R. L. Schowen, H. H. Limbach, *Can. J. Chem.* **1999**, *77*, 943–949.
[23] I. Alkorta, J. Elguero, G. S. Denisov, *Magn. Reson. Chem.* **2008**, *46*, 599–624.
[24] a) S. P. Brown, M. Pérez-Torralba, D. Sanz, R. M. Claramunt, L. Emsley, *Chem. Commun.* **2002**, 1852–1853; b) S. P. Brown, M. Perez-Torralba, D. Sanz, R. M. Claramunt, L. Emsley, *J. Am. Chem. Soc.* **2002**, *124*, 1152–1153; c) R. M. Claramunt, D. Sanz, M. Perez-Torralba, E. Pinilla, M. R. Torres, J. Elguero, *Eur. J. Org. Chem.* **2004**, 4452–4466; d) R. M. Claramunt, C. López, M. D. Santa María, D. Sanz, J. Elguero, *Prog. Nucl. Magn. Reson. Spectrosc.* **2006**, *49*, 169–206.
[25] T. N. Pham, J. M. Griffin, S. Masiero, S. Lena, G. Gottarelli, P. Hodgkinson, C. Filip, S. P. Brown, *Phys. Chem. Chem. Phys.* **2007**, *9*, 3416–3423.
[26] a) F. Cordier, S. Grzesiek, *J. Am. Chem. Soc.* **1999**, *121*, 1601–1602; b) F. Cordier, M. Rogowski, S. Grzesiek, A. Bax, *J. Magn. Reson.* **1999**, *140*, 510–512.
[27] K. Pervushin, A. Ono, C. Fernandez, T. Szyperski, M. Kainosho, K. Wüthrich, *Proc. Natl. Acad. Sci. USA* **1998**, *95*, 14147–14151.
[28] G. Cornilescu, B. E. Ramirez, M. K. Frank, G. M. Clore, A. Gronenborn, A. Bax, *J. Am. Chem. Soc.* **1999**, *121*, 6275–6279.
[29] G. Cornilescu, J. S. Hu, A. Bax, *J. Am. Chem. Soc.* **1999**, *121*, 2949–2950.
[30] C. Scheurer, R. Brüschweiler, *J. Am. Chem. Soc.* **1999**, *121*, 8661–8662.
[31] S. Grzesiek, F. Cordier, V. Jaravine, M. Barfield, *Prog. Nucl. Magn. Reson. Spectrosc.* **2004**, *45*, 275–300.
[32] J. E. Del Bene, S. A. Perera, R. J. Bartlett, *J. Am. Chem. Soc.* **2000**, *122*, 3560–3561.
[33] J. E. Del Bene, M. J. T. Jordan, *J. Am. Chem. Soc.* **2000**, *122*, 4794–4797.
[34] J. E. Del Bene, R. J. Bartlett, *J. Am. Chem. Soc.* **2000**, *122*, 10480–10481.
[35] S. A. Perera, R. J. Bartlett, *J. Am. Chem. Soc.* **2000**, *122*, 1231–1232.
[36] J. E. Del Bene, S. A. Perera, R. J. Bartlett, *Magn. Reson. Chem.* **2001**, *39*, S109-S114.
[37] J. E. Del Bene, J. Elguero, *J. Phys. Chem. A* **2006**, *110*, 7496–7502.
[38] H. H. Limbach, G. S. Denisov, N. S. Golubev, *Isotope Effects in the Biological and Chemical Sciences* (Eds.: A. Kohen, H. H. Limbach), Taylor & Francis, Boca Raton FL **2005**, Chapter 7, pp. 193–230.
[39] M. Pietrzak, J. Wehling, H. H. Limbach, N. S. Golubev, C. López, R. M. Claramunt, J. Elguero, *J. Am. Chem. Soc.* **2001**, *123*, 4338–4339.
[40] T. Glowiak, I. Majerz, Z. Malarski, L. Sobczyk, A. F. Pozharskii, V. A. Ozeryanskii, E. Grech, *J. Phys. Org. Chem.* **1999**, *12*, 895–900.
[41] A. J. Bienko, Z. Latajka, W. Sawka-Dobrowolska, L. Sobczyk, V. A. Ozeryanskii, A. F. Pozharskii, E. Grech, J. Nowicka-Scheibe, *J. Chem. Phys.* **2003**, *119*, 4313–4319.
[42] A. F. Pozharskii, *Russ. Chem. Rev.* **1998**, *67*, 1–24.
[43] V. A. Ozeryanskii, A. F. Pozharskii, A. J. Bienko, W. Sawka-Dobrowolska, L. Sobczyk, *J. Phys. Chem. A* **2005**, *109*, 1637–1642.
[44] P. Chmielewski, V. A. Ozeryanskii, L. Sobczyk, A. F. Pozharskii, *J. Phys. Org. Chem.* **2007**, *20*, 643–648.
[45] J. Klimkiewicz, L. Stefaniak, E. Grech, G. A. Webb, *J. Mol. Struct.* **1997**, *412*, 47–50.
[46] J. Klimkiewicz, M. Koprowski, L. Stefaniak, E. Grech, G. A. Webb, *J. Mol. Struct.* **1997**, *403*, 163–165.
[47] M. Pietrzak, L. Stefaniak, A. F. Pozharskii, V. A. Ozeryanskii, J. Nowicka-Scheibe, E. Grech, G. A. Webb, *J. Phys. Org. Chem.* **2000**, *13*, 35–38.
[48] M. Pietrzak, C. Benedict, H. Gehring, E. Daltrozzo, H. H. Limbach, *J. Mol. Struct.* **2007**, *844–845*, 222–231.
[49] M. Pietrzak, A. Try, B. Andrioletti, J. Sessler, P. A. Anzenbacher, H. H. Limbach, *Angew. Chem.* **2008**, *120*, 1139–1142; *Angew. Chem. Int. Ed.* **2008**, *47*, 1123–1126.
[50] G. C. Lloyd-Jones, J. N. Harvey, P. Hodgson, M. Murray, R. L. Woodward, *Chem. Eur. J.* **2003**, *9*, 4523–4535.
[51] J. E. Del Bene, I. Alkorta, J. Elguero, *Magn. Reson. Chem.* **2008**, *46*, 457–463.
[52] I. Alkorta, F. Blanco, J. Elguero, *Magn. Reson. Chem.* **2009**, *47*, 249–256.
[53] M. Grundwald-Wyspianska, M. Szafran, *J. Mol. Liq.* **1987**, *33*, 245–254.
[54] a) P. Bernatowicz, J. Kowalewski, D. Sandstrom, *J. Phys. Chem. A* **2005**, *109*, 57–63; b) P. Bernatowicz, J. Kowalewski, *J. Phys. Chem. A* **2008**, *112*, 4711–4714.
[55] S. O. Morgan, H. H. Lowry, *J. Phys. Chem.* **1930**, *34* , 2385–2432.
[56] E. F. Caldin, S. Mateo, *J. Chem. Soc. Faraday Trans. 1* **1975**, *71*, 1876–1904.
[57] a) H. Benedict, C. G. Hoelger, F. Aguilar-Parrilla, W. P. Fehlhammer, M. Wehlan, R. Janoschek, H. H. Limbach, *J. Mol. Struct.* **1996**, *378*, 11–16; b) H. Benedict, H. H. Limbach, M. Wehlan, W. P. Fehlhammer, N. S. Golubev, R. Janoschek, *J. Am. Chem. Soc.* **1998**, *120*, 2939–2950.
[58] J. L. Aubagnac, F. H. Cano, R. M. Claramunt, J. Elguero, R. Faure, M. C. Foces-Foces, P. Raj, *Bull. Soc. Chim. Fr.* **1988**, 905–908.
[59] a) M. M. King, H. J. C. M. Yeh, G. O. Dudek, *Org. Magn. Reson.* **1976**, *8*, 208–212; b) G. Martin, M. L. Martin, J. P. Gouesnard, *NMR Basic Principles and Progress, Vol. 18*, Springer, Heidelberg, **1989**.
[60] *Organikum*, 19. Aufl., **1993**, Verlag der Wissenschaften, Hamburg.
[61] C. López, P. Lorente, R. M. Claramunt, J. Marín, C. Foces-Foces, A. L. Llamas-Saiz, J. Elguero, H. H. Limbach, *Ber. Bunsenges. Phys. Chem.* **1998**, *102*, 414–418.
[62] V. A. Ozeryanskii, A. F. Pozharskii, N. V. Vistorobskii, *Russ. J. Org. Chem.* **1997**, *33*, 251–256.
[63] C. W. Rees, R. C. Storr, *J. Chem. Soc. C* **1969**, 1474–1477.
[64] A. F. Pozharskii, V. A. Ozeryanskii, *Russ. Chem. Bull.* **1998**, *47*, 66—73.
[65] A. F. Pozharskii, V. A. Kuzmenko, G. C. Aleksandrov, *Russ. J. Org. Chem.* **1995**, *31*, 570–581.
[66] K. B. Lam, J. Miller, P. J. S. Moran, *J. Chem. Soc. Perkin Trans. 2* **1977**, 457–459.
[67] We thank Professor E. Grech of Szczecin, Poland, for providing us with this process according to an unpublished procedure.

[68] M. Brookhart, B. Grant, A. F. Volpe, Jr., *Organometallics* **1992**, *11*, 3920–3922.
[69] S. Gründemann, *A Nuclear Magnetic Resonance Study of Proton Transfer Pathways in Transition Metal Complexes*, Mensch & Buch Verlag, Berlin, **2000**, pp. 33–35.
[70] N. S. Golubev, S. N. Smirnov, V. A. Gindin, G. S. Denisov, H. Benedict, H. H. Limbach, *J. Am. Chem. Soc.* **1994**, *116*, 12055–12056.

Received: August 14, 2009
Published online: December 18, 2009

